Published Online on 6 September 2017

Proc Indian Natn Sci Acad **83** No. 4 December 2017 pp. 941-948

DOI: 10.16943/ptinsa/2017/49124

Research Paper

Spectroscopy and Mineralogy of a Fresh Meteorite Fall Kamargaon (L6) Chondrite

BHASKAR J SAIKIA[1,*], G PARTHASARATHY[2], R R BORAH[3], M SATYANARAYANAN[2], R BORTHAKUR[3] and P CHETIA[4]

[1]*Department of Physics, Anandaram Dhekial Phookan College, Nagaon 782 002, India*
[2]*National Geophysical Research Institute (CSIR-NGRI), Hyderabad 500 007, India*
[3]*Department of Physics, Nowgong College, Nagaon 782 001, India*
[4]*Jorhat Science Centre and Planetarium, Jorhat 786 001, India*

(Received on 01 May 2017; Revised on 10 June 2017; Accepted on 11 August 2017)

We report spectroscopic, bulk, trace element and mineralogical composition of a fresh meteorite fall at Bali-Chapori village, near Kamargaon Town, Assam, India (26°37′56″.99 N; 93°46′ 11″.51 E) on November 13th, 2015. The whole rock analyses and the composition of olivine and pyroxene indicate that the meteorite is an ordinary chondrite belonging to the group L6. The spectroscopic (Raman, FTIR, XRD) and petrographical (HR-ICP-MS, EPMA, XRF) studies reveal that the major constituents of the meteorite is olivine [$(Mg, Fe)_2 SiO_4$], pyroxene, and metal.

Keywords: Meteorite; Spectroscopy; Mineralogy; Kamargaon; Ordinary Chondrites

Introduction

Chondritic meteorites are the oldest and most primitive rocks in the solar system. Chondrites are stony meteorites that have not been modified due to melting or differentiation of the parent body. Chondrites are broadly ultramafic in composition, consisting largely of iron, magnesium, silicon and oxygen and account for 87% of all meteorites observed to fall. The largest group of chondritic meteorites is known as the ordinary chondrites, which account for 80% of all known meteorites (Philip *et al*., 2000). Ordinary chondrites are divided into three groups, viz. H-type which have high total Fe-contents, L-type having low total Fe-contents, and LL-type having very low metallic Fe relative to the total Fe, as well as low total Fe-content. Chemical distinction among the H, L, LL-group chondrites depends on the distribution of iron between metal and silicates. It has been established that there is no or very little compositional overlap among these H, L, and LL chondrites. Changes in chemical composition (ferrous, metallic, and total iron contents and Fe/Ni ratios in the metal) is used to characterize different chondrites (Hutchison, 2004).

In this paper we report spectroscopy, composition and mineralogy of a recent meteorite fall at Bali-Chapori village (26° 37′ 56.99 N; 93° 46′ 11.51 E), near Kamargaon town in Golaghat District of Assam, India, on 13th November 2015 at 12:00 hrs (Local time). The stone was fully covered with fusion crust and had well rounded edges and well developed regmaglypts (thumbprint like impressions) on its surface, that are formed by ablation of material from the surface as a meteor passes through the Earth's atmosphere. The strike of the meteorite made an impact pit of about 40cm diameter and penetrated the ground nearly a meter in depth. A single piece of meteorite of weight 12.095 kg was recovered and has been preserved under the custody of the local police station. The fusion crust (about 1mm of thickness) and the regmaglypts are clearly visible on the surface of the meteorite (Fig. 1) (Saikia *et al*., 2017a). Five recorded falls in North-eastern region of India till date are: Assam L5 (1846), Goalpara Ureilite (1868), Sabrum LL6 (1999), Dergaon H5

**Author for Correspondence: E-mail: vaskaradp@gmail.com*

Fig. 1: A fraction of Kamargaon meteorite

(2001) and Mahadevpur H4/5 (2007) and have been documented by Grady, (2000), Ghosh *et al*. (2002); Saikia *et al*. (2007, 2008, 2009 a,b). Kamargaon is the most recent fall.

Methods

Raman spectra were collected on powdered bulk meteorite sample using a Ar^+ laser excitation source having wavelength 488 nm coupled with a Jobin-Yvon Horiba LabRam-HR Micro Raman spectrometer (equipped with an Olympus microscope with 50X objectives and a motorized x-y stage and using 1800 grooves/mm grating). The spectral resolution was around 0.1 cm^{-1} in the range from 100 to 3000 cm^{-1} and the spectra were collected with counting times of 10 to 60 s. In Raman spectra only wave numbers between 100 cm^{-1} and 1400 cm^{-1} are given due to the absence of any characteristic and significant bands between 1400 cm^{-1} and 3000 cm^{-1}.

Powdered meteorite sample was analyzed for the whole rock chemical composition by X-ray fluorescence was estimated on powdered samples using (Bhandari *et al*., 2005, 2008, 2009). The precision and accuracy of the data is ±2%, and average values of three replicates were taken for each determination. X-ray diffraction analysis was also performed on powdered sample. X-ray diffractogram was measured using a Siemens D5000 diffractometer (40 kV, 30 mA) with Cu Kα radiation ($\lambda_{K\alpha1}$ = 1.5406 Å, $\lambda_{K\alpha2}$ = 1.54439 Å), 2θ range between 15° and 65°, step size of 0.02°2θ, 1.2 s/step, divergence slit = 0.5 mm, and receiving slit = 0.3 mm.

The infrared spectrum was acquired from the homogenized spectrophotometric grade KBr and powdered meteorite pellet (1: 20) using Perkin-Elmer system 2000 FTIR spectrophotometer with helium-neon laser as the source reference and at a resolution of 4 cm^{-1}. The experimental conditions were identical to those used in studies on Dergaon and Mahadevpur meteorites (Saikia *et al*., 2009 a, b).

Quantitative mineral analyses were carried out using a JEOL JXA 8900 electron microprobe (EMPA) operated at 15 keV and a probe current of 15 nA. Natural and synthetic standards of well-known compositions were used as standards for wavelength dispersive spectrometry. The matrix corrections were made according to the $\phi\rho(z)$ procedure (Armstrong, 1991). Trace elements including rare earth (REE) and high field strength elements (HFSE) were determined by high resolution inductively coupled mass spectrometer (HR-ICP-MS) (Nu Instruments Attom®, UK) in jump-wiggle mode at resolution of 300 which permits all the element of interest to be measured accurately. The sample introduction consisted of a standard Meinhard® nebulizer with a cyclonic spray chamber housed in Peltier cooling system. All quantitative measurements were performed using the instrument software (Attolab v.2.8), while the data processing was done using Nu Quant® (Release 2.0) which uses knowledge-driven routines in combination with numerical calculations (quantitative analysis) and performs an automated or manual interpretation of the spectrum of interest. The instrument was optimized using 1ppb tuning solution and the sensitivity for ^{114}In was about 1 million cps. Oxide and oxy-hydroxide ratios were < 0.2% and the doubly charged ions ratio was < 3%. Mass bias fractionation and several well-known isobaric interferences were addressed by using certified geochemical reference materials. Precision and accuracy were better than RSD 3% for the majority of trace elements.

Results and Discussion

The petrographic investigations indicated the presence of olivine, orthopyroxene, feldspar, and opaque

minerals taenite, iron metal (kamacite) and troilite (Fig. 2A,B,C). The EPMA data (Table 1) show evidence of opaque metallic phases with kamacite and sulfide phase trolite with less than 0.4 wt % of Ni (Fig. 2A). The olivine composition is estimated to Fo = 75.50-78.98 mol %; Fa = 20.80-25.0 mol %. Kamacite Co concentrations vary systematically in various chondrite chemical groups; kamacite in H, L, LL group chondrites contain 0.4-0.5, 0.7-1.0 and 1.5-3 wt. % Co, respectively (Rubin, 1990; Reisener and Goldstein, 2003). The kamacite Co content (0.811-0.827 wt. %) in Kamargaon meteorite is similar to L group chondrites. Troilite contains < 0.4 wt % Ni, suggesting slow cooling (Smith and Goldstein, 1977). Metal and troilite occur both as separate grains and paired assemblages. Such a texture is similar to that of higher petrologic type (~6) ordinary chondrites (van Schmus and Wood, 1967). The observed opaque taenite with Ni content of 22 % confirms that Kamargaon meteorite is L6 type ordinary chondrite (Brearley and Jones, 1998). Secondary grains of feldspar with olivine are also observed. Presence of veins of feldspar and troilite exhibiting shock induced melt vein in the Kamargaon meteorite (Fig. 2B,C) is consistent with shock stage S4-S6 (Stoffler *et al*., 1991).

Table 1: Electron-Probe Micro Analysis data of Kamargaon meteorite

	Olivine (N= 20)	Pyroxene (N=12)	Feldspar (N=10)	Kamacite (N=10)
SiO_2	38.20	54.78	66.00	Fe = 92.00
Al_2O_3	—	0.10	22.20	Co = 0.70
FeO	22.40	14.12	0.10	Ni = 7.00
MnO	—	0.12	—	
MgO	39.50	30.00	—	
CaO	—	—	—	
NiO	—	0.80	2.20	
Na_2O	—	—	8.60	
K_2O	—	—	1.20	
Total	100.10	99.82	100.3	99.7

N-indicates the total numbers of grains for the EPMA analyses

Major and trace element abundances of Kamargaon meteorite sample is analyzed by X-ray fluorescence spectrometry (XRF) and high resolution inductively coupled plasma mass spectrometry (HR-ICP-MS). The results facilitated determination of the major elemental composition of Kamargaon (Table

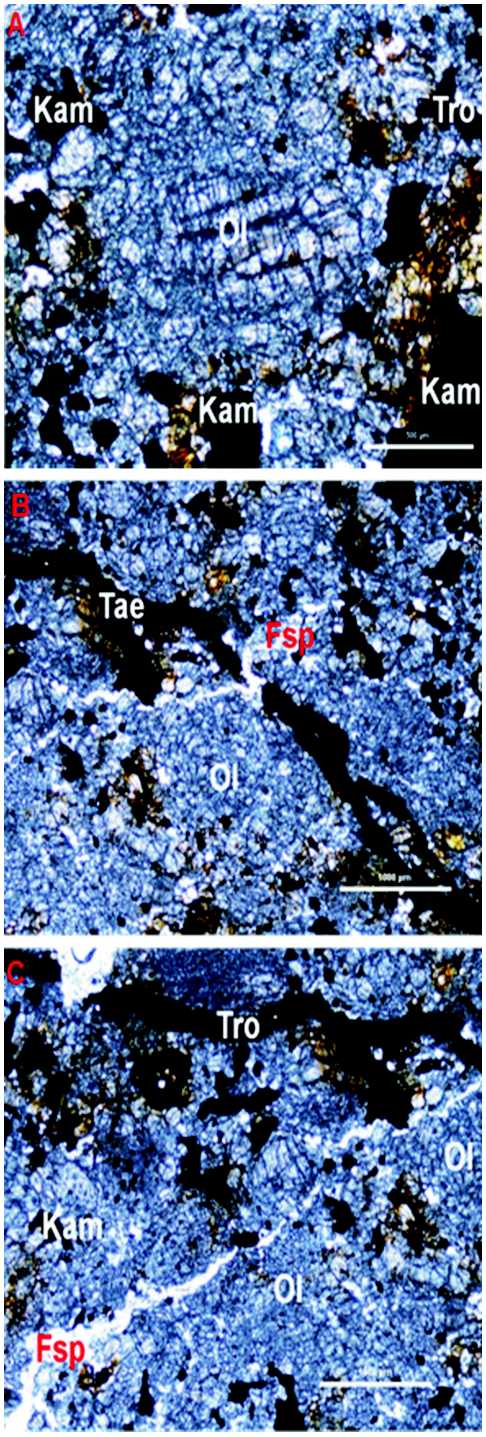

Fig. 2: (A) Thin section of Kamargaon meteorite. The olivine (Ol) composition (Fo = 78.98 to 75.5 mol%; Fa=20.80 to 25.5 mol% and Tp = 0.88 mol %) and opaque metallic phases with kamacite (Kam) and sulfide phase trolite (Tro) with Ni less than 0.4 wt%, indicative of L6 type chondrite, (B) Olivine, with feldspar (Fsp) secondary grains and opaque taenite (Tae) with Ni content of 22% confirm that Kamargaon meteorite is L6 type ordinary chondrite and (C) Veins of feldspar and troilite exhibiting shock induced melt vein in the Kamargaon meteorite

2), as well its comparison with the average values for H, L, and LL ordinary chondrites (Hutchison, 2004). Major element concentrations are typical for L-type ordinary chondrites (Table 2). Among these elements, however, the concentrations of Fe, Ni and P are significantly higher than the values in L-type ordinary chondrites. Notably, the concentration of these three elements is similar to that of H-type ordinary chondrites. In total, the abundances of 33 trace elements and rare earth elements (REEs) were determined. Elements analyzed by ICP-MS include (by increasing *Z*) Sc, V, Cr, Co, Ni, Cu, Zn, Ga, Rb, Sr, Y, Zr, Nb, Cs, Ba, all 14 REEs (La, Ce, Pr, Nd, Sm, Eu, Gd, Tb, Dy, Ho, Er, Tm, Yb, Lu), Hf, Ta, Pb, Th, and U. The REE abundance of Kamargaon is shown in Fig. 3. The Pb, Cr, Sr and Ba, abundance in Kamargaon meteorite is higher than that of H chondrites. Minor deviations from the typical values of abundances of REEs in Kamargaon, namely La, Ce and Nd, as compared to L chondrites. The total REE is 6.6 ppm and is enriched in LREE (5.9 ppm). The REE pattern shows LREE enrichment [$(La/Sm)_{cn}$ 3.6] with flat HREE [$(Tb/Yb)_{cn}$ 1.2)] and a prominent negative Eu anomaly (Eu* 0.76) indicating that plagioclase has crystallized and was removed from the melt phase prior to the formation of the rock, and that a reducing environment prevailed during the course of crystallization (Fig. 3).

Table 2: XRF derived major elemental composition of Kamargaon in relation to the composition of ordinary chondrites (H, L and LL groups) and Kaprada

Element (wt%)	H	L	LL	Kamargaon	Kaprada
Si	16.9	18.5	18.9	16.8	18.12
Ti	0.06	0.063	0.062	0.07	0.07
Al	1.13	1.22	1.19	1.28	1.2
Cr	0.366	0.388	0.374	0.382	0.3
Fe	27.5	21.5	18.5	27.2	21.5
Mn	0.232	0.257	0.262	0.280	0.24
Mg	14	14.9	15.3	14.1	15.3
Ca	1.25	1.31	1.3	1.39	1.33
Na	0.64	0.7	0.7	0.72	0.7
K	0.078	0.083	0.079	0.082	0.087
P	0.108	0.095	0.085	0.15	0.14
Ni	1.6	1.2	1.02	1.52	1.27
Co	0.081	0.059	0.049	0.066	0.06
S	2	2.2	2.3	1.93	2.27

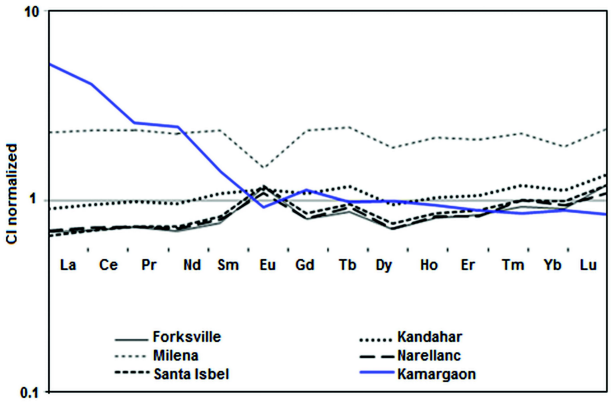

Fig. 3: Cl chondrite normalized REE pattern of Kamargaon with other L6 chondrites (Forksville, Milena, Santa Isbel, Kandahar and Narellanc)

The Fig. 4(A) reveals clear Raman lines attributable to olivine in Kamargaon meteorite. Raman bands in the region 400-800 cm^{-1} are relatively weak as compared to their infrared counterparts. Raman peaks between 700-1100 cm^{-1} are attributed to the internal stretching vibrational modes of the SiO_4 tetrahedra. In this region, the renowned doublet is found for the Si-O symmetric stretching bands at 813-823 cm^{-1} and 852-854 cm^{-1}, and a medium wave number anti symmetric Si-O stretching band appears at 965-966 cm^{-1} due to fosterite (F_o). The peaks of the 813-852 cm^{-1} doublet is assigned to a mixed contribution of the symmetric ($\nu 1$) and asymmetric ($\nu 3$) stretching modes of Si-O_{nb} bonds (Non-Bridge Oxygen, NBO) in SiO_4 tetrahedra (Lam *et al.*, 1990). Raman spectra indicates the characteristic doublet at 822.06 cm^{-1} and 851.79 $cm^{-1}$from the coupling between the symmetric ($\nu 1$) and anti symmetric ($\nu 3$) stretching modes of Si-O_{nb} bonds in SiO_4 tetrahedra of olivine (Saikia *et al.*, 2016, 2017b). This peak position may shift upwards as the values of F_o increase (Chopelas, 1991). The F_o value of an olivine can be determined from the compositional results. The F_o value of a meteorite corresponds to forsteritic olivines, with about 27.20% of Fe. The low wave number peak at 572.14 cm^{-1} occurs due to the bridging oxygen (BO). The medium wave number peak at 916.92 cm^{-1} indicates polymerization. The 822.06 cm^{-1} peak has a higher contribution of $\nu 3$ (asymmetric mode) than the 851.79 cm^{-1} peak. This mode is more easily affected by variations in the Si-O_{nb} force constant, and is also affected by the breakdown of SiO_4 during polymerization (Lam *et al.*, 1990). Relative peak height depends on crystal orientation (Ishii, 1978). Therefore,

systematic variations of high-wave number Si-O bands are attributed to decreased distortion of SiO_4 tetrahedra. A weak band at 712 and 918 cm^{-1} corresponds to wadsleyite (Chen *et al*., 2004). Table 3 represents a comparison of Kamargaon data with theoretical Raman peak positions of different class of ordinary chondrites by Pittarello *et al*. (2015). Raman peaks (Fig. 4A and B) of Kamargaon at 822.06 cm^{-1} and 851.79 cm^{-1} are due to olivine. Peaks at 337.12 cm^{-1}, 680.45 cm^{-1} and 1006.13 cm^{-1} due to pyroxene is identical to the values for L-chondrites (Pittarello *et al*. 2015). The full width at half maximum (FWHM) values of the *v*1 olivine band in the Raman spectra of L6 ordinary chondrites have been related to the degree of crystal structural disorder resulting from shock deformation (Miyamoto & Ohsumi, 1995), and range from 10 cm^{-1} to 21 cm^{-1} for poorly shocked to strongly shocked meteorites respectively. The observed FWHM value of the olivine Raman line at 822.06 cm^{-1} (*v*1) is ~17 cm^{-1} and is identical to the strongly shock stage. The Raman spectral pattern of end-member chromite (Fig. 4B) consists of a major broad peak near 684 cm^{-1} and a shoulder near 650 cm^{-1}. Other minor peaks are seen at 639, ~615, ~518, ~478 and ~432 cm^{-1}. The strongest peak at 684 cm^{-1} is assigned to the A_{1g} mode and this feature presumably is generated by the bonds in (Cr^{3+}, Fe^{3+}, Al^{3+})O_6 octahedra. The trivalent ions lead to a more compact structure and a higher degree of covalency than those in $Fe^{2+}O_4$ tetrahedra (Wang *et al*., 2004a). Strong fluorescence at 400-520 cm^{-1} could hide the intense feldspar Raman bands at around 500 cm^{-1}. On the other hand, FeNi metal has no active modes for Raman spectroscopy and troilite is a weak Raman scatterer (Wang *et al*., 2004b).

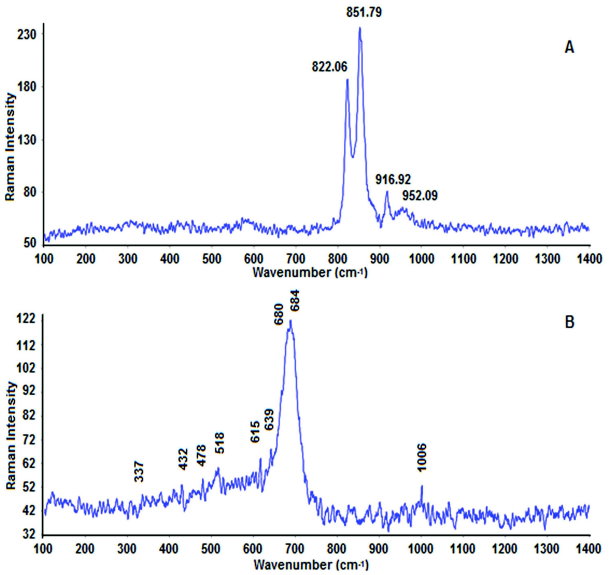

Fig. 4: Raman spectra of the olivine (A) and chromite (B) recorded in the spectral region 100-1400 cm^{-1} from different points of Kamargaon meteorite

The infrared spectrum of Kamargaon (Fig. 5) reveals numerous absorption bands in 800-1150 cm^{-1} and 400-700 cm^{-1} region indicating the presence of silicates in the sample. These band profiles generally depend on the crystalline structure of the silicates and can therefore be used to identify the mineral phases. The absorption features in the decreasing intensities in the Si-O stretching region and the Si-O-Si bending vibrations at 1057, 926, 904 and 508 cm^{-1} is identical to the bands of fayalite (Fe_2SiO_4) (F_a 20.80), the bands found at 995, 884, 839, 616, 548 and 508 cm^{-1} are identical to the bands of forsterite (Mg_2SiO_4) and the bands found at 1057, 972, 913, 874 and 533 cm^{-1} are identical to the bands of enstatite (Mg_2SiO_3)

Table 3: Comparison of Kamargaon Raman peak positions with the chemical group attribution based on theoretical Raman peak position by Pittarello *et al.* (2015)

Chemical group		Peak A(cm^{-1})	Peak B(cm^{-1})	Peak C(cm^{-1})
H	$Fa_{16–20}$	821.9–822.3	852.5–853.4	—
	$Fs_{14–18}$	337.9–339.5	681.2–682.5	1007.8–1009.0
L	$Fa_{22–26}$	821.3–821.7	851.2–852.1	—
	$Fs_{19–22}$	336.5–337.6	679.9–680.8	1006.6–1007.5
LL	$Fa_{26–32}$	820.6–821.3	849.9–851.2	—
	$Fs_{22–26}$	334.9–336.5	678.6–679.9	1005.5–1006.6
Kamargaon	$Fa_{20.8–25.0}$	822.06	851.79	—
	$Fs_{20.4–21.2}$	337.12	680.45	1006.13

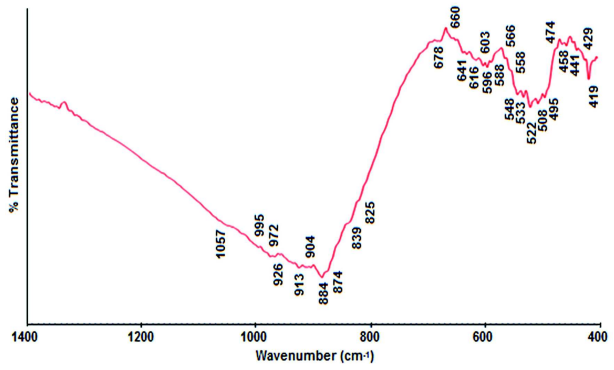

Fig. 5: The infrared spectra of Kamargaon meteorite in the spectral region 1400-400 cm^{-1}, olivine is recorded in 1000-500 cm^{-1} region

(Gadsden, 1975; Saikia *et al.* 2011). The observed band at 508 cm^{-1} can be interpreted as Si-O and Mg-O vibration modes in enstatite ($MgSiO_3$) with slight shifts in the matrix (Nakamoto, 1978). The Si-O asymmetric stretching vibration (TO2-T2O5) is observed in between the peaks 995-1057 cm^{-1}. The observed peak positions 913-972 cm^{-1} and 874-884 cm^{-1} are arises due to the Si-O asymmetric vibration (TO3) and (T2O7- -TO4) respectively. In the bending vibration region, the peak at 687 cm^{-1} is arises due to the symmetrical bending vibration of O-Si (Al)-O. The Si-O-Si bending vibrations are observed in between 458-495 cm^{-1}.

The powder X-ray diffraction pattern (Fig. 6) shows major phases of pyroxenes (enstatite); olivine (forsterite) and iron (kamacite). The most abundant mineral in Kamargaon meteorite is olivine, followed by pyroxene (enstatite), and iron (kamacite). The peaks (420), (321) and (610) at 28.09º, 30.31º, and 31.09º, correspond to Ca-poor orthopyroxene, Ca-poor clinopyroxene, and Ca-rich pyroxene phases respectively. The orthopyroxene peak (321) at 30.31º is an indicator of equilibrated chondrite. Generally, the height of peak around 31º is highest among these three peaks for the equilibrated ordinary chondrite. In this range, the diffraction pattern of Kumargaon exhibits the highest peak at 31.09º (Fig. 6). Other pyroxene (enstatite) peaks are observed at 41.74º, 46.06º, 54.70º, 56.62º, 61.78º and 62.44º. The peak (110) appears at 44.47º is due to kamacite [$\propto$-(Fe, Ni)]. The other peaks observed at 17.32º, 22.81º, 25.36º, 32.23º, 35.59º, 36.46º, 39.61º and 52.12º are reveals the presence of olivine (forsterite). The X-ray diffraction pattern also confirms of fayalite rich olivine.

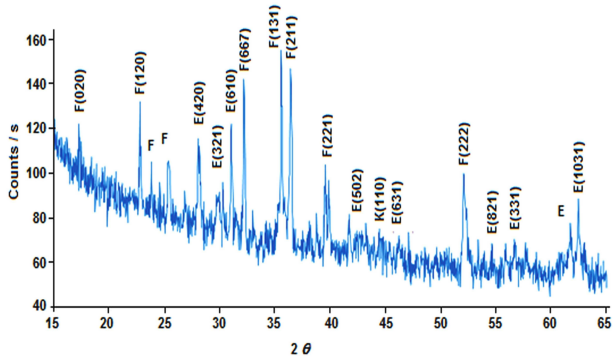

Fig. 6: X ray diffraction pattern of Kamargaon meteorite (F: forsterite, E: enstatite, K: kamacite)

Conclusion

This study represents spectroscopic, compositional and mineralogical investigations of Kamargaon meteorite. The electron-probe microanalysis indicates that the Kamargaon meteorite is an L6 chondrite. The Raman analysis is consistent with the electron-probe microanalysis results. Raman spectral pattern reveals chromite as an end-member. FeNi metal has no active modes for Raman spectroscopy and troilite is a weak Raman scatterer. Following an alternative classification using Raman spectroscopy by Pittarello *et al.* (2015), the Raman peak positions due to olivine and pyroxene of Kamargaon are identical to the L-chondrites. Observed FWHM value of the olivine Raman line at 822.06 cm^{-1} (ν1) is ~17 cm^{-1}, which is identical to the strongly shocked stage. Compositional and trace elements abundances show good agreements with L. chondrite. A prominent negative Eu anomaly indicates partial melting or fractional crystallization of the source. X-ray diffraction pattern indicates that the most abundant mineral in Kamargaon meteorite is olivine (d = 2.4567 Å), followed by pyroxene (d = 2.8700 Å), and kamacite (d = 2.0280 Å). The diffraction peak of orthopyroxene at 30.31º indicates it to be an equilibrated chondrite. Phases of olivine (forsterite) and pyroxenes (enstatite) are also characterized by infrared spectroscopy. The overall spectroscopic analysis of Kamargaon is consistent with the geochemical compositional analysis. While this manuscript was under review, a report on the fall of the Kamargaon meteorite has been reported by Ray *et al.* (2017). Our present study confirms the classification of the meteorite as L6 chondrite.

Acknowledgements

This paper is dedicated to 80th Birthday of Professor E S Raja Gopal, Department of Physics, Indian Institute of Science, Bangalore. We thank, Directors, National Geophysical Research Institute (NGRI), Hyderabad and Indian Institute of Technology, Guwahati (IITG) for analytical facilities; Professor Laurence Garvie for useful discussion. We are grateful to the Editor Dr. A K Singhvi and the anonymous reviewers for their constructive comments. We thank PLANEX program, PRL, and Space Application Centre, Department of Space, Government of India, for their valuable support. We also thank to Dr. S Sarmah, IIT Guwahati, and Dr. J R Chetia, Dibrugarh University for their assistance with the spectroscopic analysis.

References

Armstrong J T (1991) Quantitative elemental analysis of individual microparticles with electron beam instruments. In Heinrich K. F. J. and Newbury D. E. (Ed.) Electron probe quantitation, Plenum Press, New York, 261-315 pp

Bhandari N, Murty S V S, Shukla P N, Mahajan R R, Shukla A D, Suthar K M, Parthasarathy G and Paliwal B S (2005) Bhawad LL6 chondrite: chemistry, petrology, noble gases, nuclear tracks and cosmogenic radionuclides in *Meteorit Planet Sci* **40** 1015-1022

Bhandari N, Murty S V S, Shukla P N, Mahajan R R, Shukla A D, Lashkari G, Sisodia M S, Tripati RR, Parthasarathy G, Verma H C and Franchi I A (2008) Aarki (L5) chondrite: first meteorite find in Thar desert of India in *Meteorit Planet Sci* **43** 761-770

Bhandari N, Murty S V S, Mahajan R R, Parthasarathy G, Shukla P N, Sisodia M S and Rai V K (2009) Kaprada (L5/6) chondrite: chemistry, petrography, noble gases, and nuclear tracks in *Planet Space Sci* **57** 2048-2052

Brearley A J and Jones R H (1998) Reviews in mineralogy and geochemistry in *Rev Min* **36** 398

Chen M, Ahmed El Goresy A E and Gillet P (2004) Ringwoodite lamellae in olivine: Clues to olivine-ringwoodite phase transition mechanisms in shocked meteorites and subducting slabs in *PNAS* **101** 15033-15037

Chopelas A (1991) Single crystal Raman spectra of forsterite, fayalite, and monticellite in *Am Mineral* **76** 1101-1109

Gadsden J A (1975) Infrared spectra of Mineral and related Inorganic Compounds. Butterworths, USA, 160-175pp

Grady M M (2000) Catalogue of meteorites. Cambridge University Press, Cambridge, UK

Ghosh S, Murty S V S, Shukla P N, Shukla A D, Mahajan R R, Bhandari N. Pant N C, Ghosh J B and Shome S (2002) Fall, classification and cosmogenic records of the Sabrum(LL6) chondrite in *Meteorit Planet Sci* **37** 439-448

Hutchison R (2004) Meteorites: a Petrologic, Chemical, and Isotopic Synthesis. Cambridge University Press, Cambridge, UK, 506 pp

Iishi K (1978) Lattice dynamics of forsterite in *Am Mineral* **63** 1198-1208

Lam P K, Yu R, Lee M W and Sharma S K (1990) Relationship between crystal structure and vibrational mode in Mg_2SiO_4 in *Am Mineral* **75** 109-1l9

Miyamoto M and Ohsumi K (1995) Micro Raman spectroscopy of olivines in L6 chondrites: Evaluation of the degree of shock in *Geophys Res Lett* **22** 437-440

Nakamoto K (1978) Infrared and Raman Spectra of Inorganic and Coordination Compounds, John Wiley and Sons, New York, 105-139 pp.

Philip A B, Alex W R B and Tim Jull A J (2000) Ancient Meteorite Finds and the Earth's Surface Environment in *Quat Res* **53** 131-142

Pittarello L, Baert K, Debaille V and Claeys P (2015) Screening and classification of ordinary chondrites by Raman spectroscopy in *Meteorit Planet Sci* **50** 1718-1732

Ray D, Mahajan R R, Shukla A D, Goswami T and Chakraborty S (2017) Petrography, classification, oxygen isotopes, noble gases, and cosmogenic records of Kamargaon (L6) meteorite: The latest fall in India in *Meteorit Planet Sci* **52** 1744-1753

Reisener R J and Goldstein J I (2003) Ordinary chondrite metallography, Part 2. Formation of zoned and unzoned metal particles in relatively unshocked H, L and LL chondrites in *Meteorit Planet Sci* **38** 1679-1696

Rubin A E (1990) Kamacite and olivine in ordinary chondrites: Intergroup and intragroup relationships in *Geochim Cosmochim Acta* **54** 1217-1232

Rubin A E (2005) Relationships among intrinsic properties of ordinary chondrites: Oxidation state, bulk chemistry, oxygen-isotopic composition, petrologic type and chondrule size in *Geochim Cosmochim Acta* **69** 4907-4918

Saikia B J, Parthasarathy G, Sarmah N C and Baruah G D (2007) Organic compounds in H5 meteorite: Spectroscopic investigation of Dergaon H5 chondrite in *Geochim*

Cosmochim Acta **71** A867

Saikia B J and Parthasarathy G (2008) Spectroscopy of Dergaon meteorite in *Geochim Cosmochim Acta* **72** 818

Saikia B J, Parthasarathy G and Sarmah N C (2009a) Fourier transform infrared spectroscopic characterization of Dergaon H5 chondrite: Evidence of aliphatic organic compound in *Nat Sci* **7** 45-51

Saikia B J, Parthasarathy G and Sarmah N C (2009b) Spectroscopic characterization of olivine [$(Fe, Mg)_2SiO_4$] in Mahadevpur H4/5 ordinary chondrite in *J Am Sci* **5** 71-78

Saikia B J, Parthasarathy G and Borah R R (2011) Spectroscopic characterization of olivine due to Fe/Mg in Dergaon chondrite in *Mineral Mag* **75** 1780

Saikia B J, Parthasarathy G, Borah R R and Borthakur R (2016) Raman spectroscopic study of Dergaon H5 and Mahadevpur H4/5 chondrite in *47th Lunar and Planetary Science Conference*.#1799

Saikia B J, Parthasarathy G and Borah R R (2017a) Raman spectroscopy of Kamargaon L6 ordinary chondrite in *48th Lunar and Planetary Science Conference*.#1979

Saikia B J, Parthasarathy G and Borah R R (2017b) Nanodiamonds and silicate minerals in ordinary chondrites as determined by micro-Raman spectroscopy in *Meteorit Planet Sci* **52** 1146-1154

Smith B A and Goldstein J I (1977) The metallic microstructures and thermal histories of severely reheated chondrites in *Geochim Cosmochim Acta* **41** 1061-1072

Stoffler D, Keil K and Scott E R D (1991) Shock metamorphism of ordinary chondrites in *Geochim Cosmochim Acta* **55** 3845-3867

vanSchmus W R and Wood J A (1967) A chemical-petrologic classification for the chondritic meteorites in *Geochim Cosmochim Acta* **31** 747-765

Wang A, Kuebler K E, Jolliff B L and Haskin L A (2004a) Raman spectroscopy of Fe-Ti-Cr-oxides, case study: Martain meteorite EETA79001 in *Am Mineral* **89** 665-680

Wang A, Kuebler K, Jolliff B and Haskin L A (2004b) Mineralogy of a Martian meteorite as determined by Raman spectroscopy in *J Raman Spectros* **35** 504-514.